Available online at www.sciencedirect.com
SCIENCE DIRECT®

Nuclear Engineering and Design 236 (2006) 1282–1292

Nuclear Engineering and Design

www.elsevier.com/locate/nucengdes

Prediction of flooding gas velocity in gas–liquid counter-current two-phase flow in inclined pipes

Akiharu Ousaka [a,*], Deendarlianto [b], Akira Kariyasaki [c], Tohru Fukano [d]

[a] Department of Mechanical Engineering, The University of Tokushima, 2-1 Minami-josanjima, Tokushima 770-8506, Japan
[b] Graduate School of Engineering, The University of Tokushima, 2-1 Minami-josanjima, Tokushima 770-8506, Japan
[c] Department of Chemical Engineering, Fukuoka University, 8-19-1 Jyonan-ku, Fukuoka 814-0180, Japan
[d] Department of Mechanical Engineering, Kurume Institute of Technology, 2228-66 Kamitsu, Kurume, Fukuoka 830-0052, Japan

Received 26 September 2005; received in revised form 12 December 2005; accepted 12 December 2005

Abstract

The purpose of the experimental study is to investigate the effects of pipe inclination, pipe length, pipe diameter and surface tension of the working liquid on the onset of flooding of gas–liquid adiabatic counter-current two-phase flow in inclined pipes. Flooding in inclined pipes were observed by using the combination of visual observation, measurement of discharged liquid flow rate and time variation of liquid hold-up. And it was defined as the maximum air flow rate at which the discharged liquid flow rate is equal to the inlet liquid flow rate. As a result we proposed a correlation to predict the flooding gas velocity in inclined pipes under a given liquid flow rate, and the predictions agreed well with the experimental observations.

1. Introduction

Counter-current gas–liquid two-phase flow in an inclined pipe has been encountered in a diverse range of process industries. Particularly in Japan PWRs, for example, in the emergency core cooling (ECC), the cold water will be injected into the reactor through an inclined pipe during a loss of coolant accident (LOCA). At this condition it is considered that the reactor will be depressurized, and vaporization takes place. Therefore, saturated steam is generated in the reactor core, and rushes out of the inclined pipe. Consequently a stratified counter-current flow of steam and cool water occurs. However, the cool water cannot penetrate into the core and cooling will not take place if the out-going steam flow causes flooding.

An understanding of flooding is of considerable technological importance, because it limits important operational parameters of such an equipment. That is, the flooding leads to complex thermo-fluid dynamic processes that include condensation of steam due to the introduction of cold water into the reactor core. Various types of pipe length, pipe inclination and inner diameter are used in this appliance. However, among the many reports on flooding phenomena in inclined pipes (for example, Barnea et al., 1986; Mouza et al., 2003; Fiedler and Auracher, 2004) few considered the above parameters in their studies.

The effects of pipe inclination on the flooding gas velocity were examined by Hewitt (1977), Barnea et al. (1986) and Mouza et al. (2003). Hewitt used the pipe inclination angles from 10° to 90° to horizontal, and noticed that the inclination angle of the pipe influenced the both phase's velocities of the onset of flooding significantly, but not systematically. This result was confirmed by Barnea et al. (1986). Recently, Mouza et al. (2003) also performed flooding experiments in inclined pipes. The pipe inclinations ranged from 30° to 60° to horizontal. They reported that the flooding gas velocity decreases as the pipe inclination increases, and the flooding gas velocity by Barnea et al. (1986) tends to be significantly higher than their data. Next, Mouza et al. also used water–air and kerosene–air as the working fluids to examine the effect of liquid properties on flooding in inclined pipes, and noticed that the flooding gas velocity of kerosene is lower than that of water. Thus the effects of the other parameters such as pipe length and surface tension on flooding in inclined pipes have not been investigated.

In case of vertical pipe, the investigations on the effects of pipe length and surface tension on flooding were performed in

* Corresponding author. Tel.: +81 88 656 7375; fax: +81 88 656 9082.
E-mail address: ousaka@me.tokushima-u.ac.jp (A. Ousaka).

0029-5493/$ – see front matter
doi:10.1016/j.nucengdes.2005.12.001

Nomenclature

C	constant in Eq. (2)
C_K	constant in Eq. (4)
C_1, C_2	constants in Eq. (5)
D	pipe diameter (m)
D_e	hydraulic diameter (m)
D^*	dimensionless pipe diameter
Fr_L	liquid Froude number
g	gravitational acceleration (m/s^2)
h	wave height (m)
J_G	superficial gas velocity (m/s)
J_{GF}	superficial flooding gas velocity (m/s)
J_L	superficial liquid velocity (m/s)
J_K^*	Wallis dimensionless number of superficial velocity
K_K^*	Kutateladze dimensionless number of superficial velocity
L	pipe length (m)
m	constant in Eq. (2)
Oh_L	Ohnesorge number
Re_{GF}	gas Reynolds number at the onset of flooding
Re_K	Reynolds number of gas or liquid
t	time (s)
Δv	relative velocity between gas and liquid (m/s)
We	Weber number
x	distance from the liquid outlet (m)
Greek letters	
η	liquid hold-up
θ	inclination angle to horizontal (°)
μ	viscosity (Pa s)
ρ_k	density of gas or liquid (kg/m^3)
σ	surface tension (N/m)

the past, but those effects are still unclear. It was pointed out by Suzuki and Ueda (1977) that the flooding gas velocity decreased with increasing pipe length. This was confirmed by McQuilland and Whalley (1985). In addition, Suzuki and Ueda also noted that the effect of pipe length was small in a range of low liquid flow rates but significant in a range of high liquid flow rates. Recently, Jeong and No (1996) reported that the effect of pipe length was significant only when the entrance and exit geometry were smooth. However, it has not been always recognized. In fact, Dukler et al. (1984) reported that the flooding gas velocity was independent of pipe length.

The effect of surface tension on the flooding gas velocity in vertical pipes is also still unclear. Chung et al. (1980) reported that the surface tension had a stabilizing effect on flooding, i.e., the flooding gas velocity decreased with a decrease in the surface tension. English et al. (1963) also found the same trend, but not Kamei et al. (1954). On the other hand, Suzuki and Ueda (1977) reported that the effect of surface tension was complicated and the flooding gas velocity took its maximum value at the surface tension close to 5.0×10^{-2} N/m.

The present authors have already reported on the detailed liquid film behavior at the onset of flooding in an adiabatic counter-current air–water two-phase flow in an inclined pipe (Deendarlianto et al., 2005a). They clarified two mechanisms at the onset of flooding, lower flooding and upper flooding. The term of "lower flooding and upper flooding" indicates the location where the flooding is initiated respectively at the lower or the upper part of the test section. The lower flooding occurs in lower liquid flow rates and high pipe inclination angles, and the breakdown of the wave occurs in the lower part of the pipe (x/L ranged from 0.0 to 0.5). Here, L means the total pipe length and x is the distance from liquid outlet. The breakdown of waves is considered as the onset of flooding because all the liquid supplied cannot flow down smoothly in this situation. It is initiated by the increase in the wave height, in which the wave formation begins at the upper part of the test pipe ($x/L \cong 1.0$). The wave height increases with the downward movement. It will be broken by the airflow when the wave height reaches a certain height in counter-current flow. The liquid droplets arise nearly at the same time of the breakdown of the wave. Even in this moment there is no upward motion of the wave.

On the other hand, the upper flooding occurs at higher liquid flow rate and low pipe inclination. It is initiated by the formation of a liquid slug in the upper part of the test pipe ($x/L \cong 1.0$), in which the maximum of liquid hold-up is approximately 1.0. This means that the liquid lump completely blocks the overall cross section of the test pipe. It moves downward for quite short distance with the instantaneous increase of gas inlet pressure, and will be broken by airflow in the upper part of the test pipe (x/L from 0.5 to 1.0). However, a reliable method to predict gas velocity at the onset of flooding in inclined pipes has not been given.

The purpose of the present study is to investigate the effects of pipe inclination, pipe length, pipe diameter and surface tension of the working fluid on the onset of flooding, and to propose a correlation to predict the flooding gas velocity in inclined pipes. In the present paper, the experimental results on the influence of fundamental parameters will be presented first. Next, the existing correlations will be evaluated briefly. Finally, we will propose a new correlation.

2. Experimental apparatus and procedures

A schematic diagram of the present experimental apparatus is shown in Fig. 1. It consisted of four counter-current flow pipes having total lengths of 0.5, 1.1, 2.2 and 5.5 m, respectively. Air from a compressor was introduced from the lower end of the inclined pipe and flowed upward through the test section to a separator, S. Liquid measured by a digital flow meter entered into the test pipe from a porous section and flowed downward in the pipe. To ensure the accuracy, the liquid flow rate was confirmed by collecting the liquid discharged from the outlet, i.e., the lower end of the test pipe over a fixed period of time.

Each pipe was made of transparent acrylic resin to permit the visual observation of flow behavior in the pipe. The inner diameters of the test pipes were 16 and 26 mm. The liquid inlet consisted of a porous tube in order to make the inlet liquid film

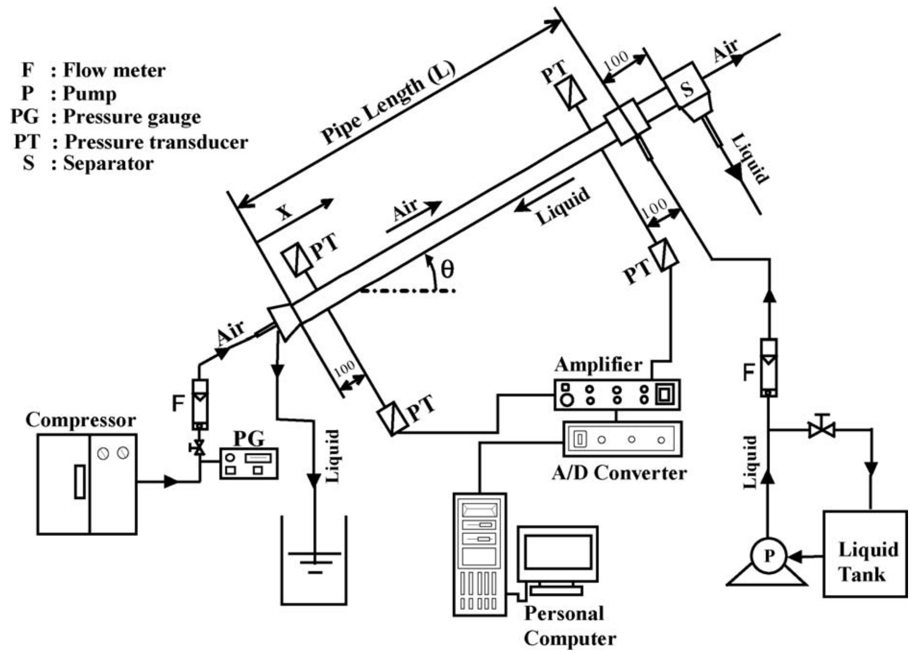

Fig. 1. Schematic diagram of experimental apparatus.

flow circumferentially uniform. The air entrance section was made of acrylic resin, providing a conical inlet passage in order to avoid the turbulence effect in this section (Deendarlianto et al., 2002, 2004, 2005a)

The experiments were performed using air and three test liquids, i.e., water and aqueous oleic acid natrium solution of two different concentrations, thus providing test liquids with a variation of surface tension, σ_L. The liquid temperature was about ambient temperature, i.e., ≈20 °C and their properties are given in Table 1, where ρ_L is the density of liquid, σ_L the surface tension and μ_L is the viscosity. The liquid surface tension was measured by the automatic surface tension measurement system with satisfactory accuracy and reproducibility (Matsuki et al., 1994, 1999). In the present study, the measurements of surface tension were done both at the inlet and the exit of test pipe, before and after the experiment. As a result the values of surface tension were almost the same. This indicates the concentration and distribution of surfactant in the test fluids are almost uniform. Consequently, the effect of dynamic surface tension in our experiments can be neglected.

In the present study, we used oleic acid natrium to decrease the surface tension of water because it is a powerful surfactant which, when used in low concentrations (0.1 wt.%), decreases the surface tension to 0.031 N/m without affecting other liquid properties. The measured relationship between the surface tension and the weight percentage of oleic acid natrium is shown in Fig. 2.

The flow behavior was recorded by two high-speed video cameras with a speed of 240 frames/s and a shutter speed of 1/10,000 s. The instantaneous local hold-up was detected using the constant electric current method (CECM). In the present study, we used many liquid hold-up sensors arranged along the pipe. The output signals from the sensors were sent respectively through amplifiers with high input impedance to a personal computer via an A/D converter. The liquid hold-up data were acquired at a sampling rate of 1.0 kHz. The details of the principle, equipment, measuring system and calibration method can be found in Fukano (1971, 1998).

The experimental conditions were as follows—pipe inclination angles: 30°, 45° and 60° to horizontal; the range of superficial liquid velocity: $J_L = 0.03$–0.32 m/s; and that of air:

Table 1
Physical properties of liquid used in the experiment (at 20 °C)

Tested liquid	ρ_L (kg/m^3)	σ_L (N/m)	μ_L (Pa s)
Water (S72)	998.2	0.072	10.03×10^{-4}
0.02 wt.% oleic acid natrium solution (S51)	998.2	0.051	10.03×10^{-4}
0.05 wt.% oleic acid natrium solution (S34)	998.2	0.034	10.03×10^{-4}

ρ_L, density; σ_L, surface tension; μ_L, static viscosity.

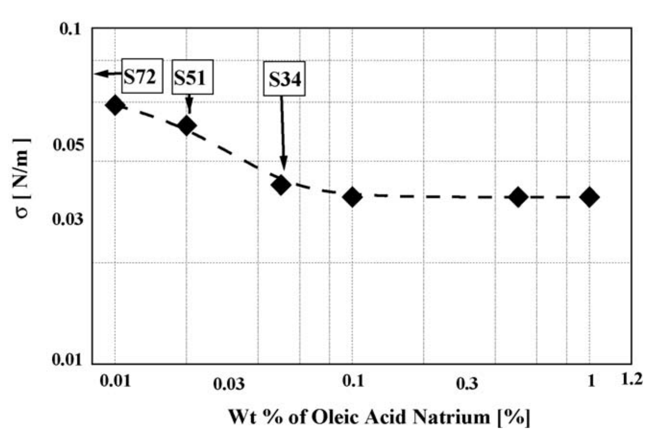

Fig. 2. Surface tension vs. weight percentage of oleic acid natrium (at 20 °C).

Table 2
Experimental condition

Pipe length, L (m)	Pipe diameter, D (mm)	Pipe inclination, θ (°)	Fluid
0.5	16	30, 45, 60	S72
1.1	16	30, 45, 60	S72, S51, S34
2.2	16	30, 45, 60	S72
5.5	16	30, 45, 60	S72, S51, S34
5.5	26	30, 45, 60	S72

$J_G = 0.0$—14 m/s. Designation of experimental data sets is summarized in Table 2. For the sake of brevity, we use some abbreviations for the test liquids, i.e., S72: air–water (static surface tension of liquid $\sigma_L = 0.072$ N/m); S51: air–0.02 wt.% aqueous oleic acid natrium solution ($\sigma_L = 0.051$ N/m); and S34: air–0.05 wt.% aqueous oleic acid natrium solution ($\sigma_L = 0.034$ N/m).

3. Results and discussion

3.1. Discharged liquid flow rate

In the present experiment, the liquid flow rate was kept constant and the airflow rate was increased by small increments from zero, i.e., the flow pattern was the free falling film at the first stage. We waited for a few minutes to ensure the flow pattern became in a steady state after the change of the airflow rate. Next, the liquid hold-up, pressure gradient and discharged liquid flow rate were recorded. The onset of flooding was defined as the limit of stability of the counter-current flow, which was identified by the maximum airflow rate at which the discharged liquid flow rate is equal to the inlet liquid flow rate.

The typical results of flooding curves are shown in Fig. 3, in which (a), (b) and (c) correspond to the cases of S72, S51 and S34, respectively. The pipe length and pipe inclination were respectively $L = 1.1$ m and $\theta = 30°$, as an example. In the figure, the abscissa indicates the superficial air velocity J_G and the ordinate the discharged superficial liquid velocity $J_{L,D}$ at the liquid outlet. The onset of flooding is marked by the arrows in each line of constant supplied liquid flow rate, J_L. The point in which the discharged superficial liquid velocity $J_{L,D}$ becomes zero is defined as the zero liquid penetration, marked as ZP in the figure. The region between the onset of flooding and ZP is defined as the partial delivery region.

Fig. 3 reveals that in the partial delivery region the discharged superficial liquid flow rate $J_{L,D}$ decreases gradually and becomes zero at ZP. Those trends of $J_{L,D}$ against J_G were almost same regardless of the inlet liquid flow rate, i.e., the data points in that region fall almost on one line. Here, consider the role of liquid film and liquid droplet to upward transportation. In the present study, it was considered that the entrainment of liquid droplet were responsible of the reduction of the downward liquid flow rate (Deendarlianto et al., 2005a,b). This result agrees well with that obtained by Zabaras and Dukler (1988) who showed a gradual decrease in the discharged liquid flow rate in the partial delivery region for 1.0 M solution

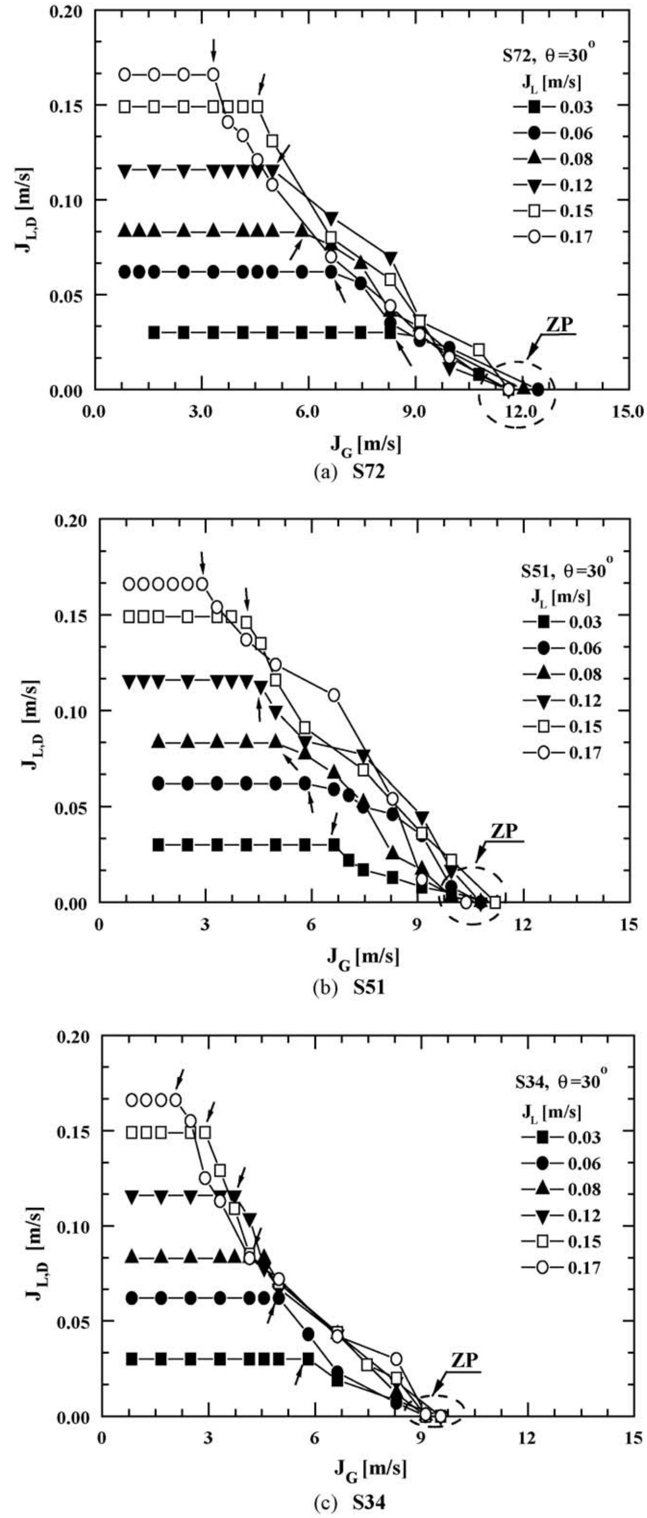

Fig. 3. Discharged superficial liquid velocity vs. superficial air velocity ($L = 1.1$ m and $\theta = 30°$).

of NaOH. On the other hand it has a contradiction to the result obtained by Clift et al. (1966) who reported that the down flow rate drops immediately, therefore, the upward movement of the liquid slug was responsible for the upward liquid transportation. The volume of the liquid transported by the liquid slug is much higher than the entrainment liquid droplets. Therefore, a sudden drop of discharged liquid flow rate occurred in their experiment.

3.2. Effect of fundamental parameters on the flooding gas velocity

3.2.1. Effect of pipe inclination

The typical result of pipe inclination effect on the flooding gas velocity is shown in Fig. 4(a)–(c) for the cases of S72, S51 and S34, respectively. In the figure, the flooding gas velocity J_{GF} is plotted against the pipe inclination θ with the supplied inlet superficial liquid velocity J_L as a parameter. The pipe length L is 1.1 m, as an example. As shown in this figure, the trend of J_{GF} against θ is complicated. That is, J_{GF} takes the maximum value at about $\theta = 45°$ in the region of low J_L, while it takes the maximum value at $\theta = 60°$ in the higher J_L condition. In the previous work, the present authors (Deendarlianto et al., 2005a) compared J_{GF} in an inclined pipe with $L = 2.2$ m with that in the vertical pipe. The data of vertical pipe were calculated from the correlation proposed by Wallis (1969). The comparison showed that J_{GF} of vertical pipe is lower than that of $\theta = 60°$. From this comparison and the present experimental data, it is possible to conclude that J_{GF} increases and after taking maximum value it decreases as the pipe inclination is increased from horizontal to vertical. The observed trend in the present research confirms them reported by Hewitt (1977), Barnea et al. (1986) and Celata et al. (1992).

In the previous paper (Deendarlianto et al., 2005a), it was reported that pipe inclination also has a significant effect on the flooding mechanisms. The lower flooding moves to upper flooding as the pipe inclination decreases. This means that the blockage with liquid lump as a characteristic of upper flooding disappears as the pipe inclination increases.

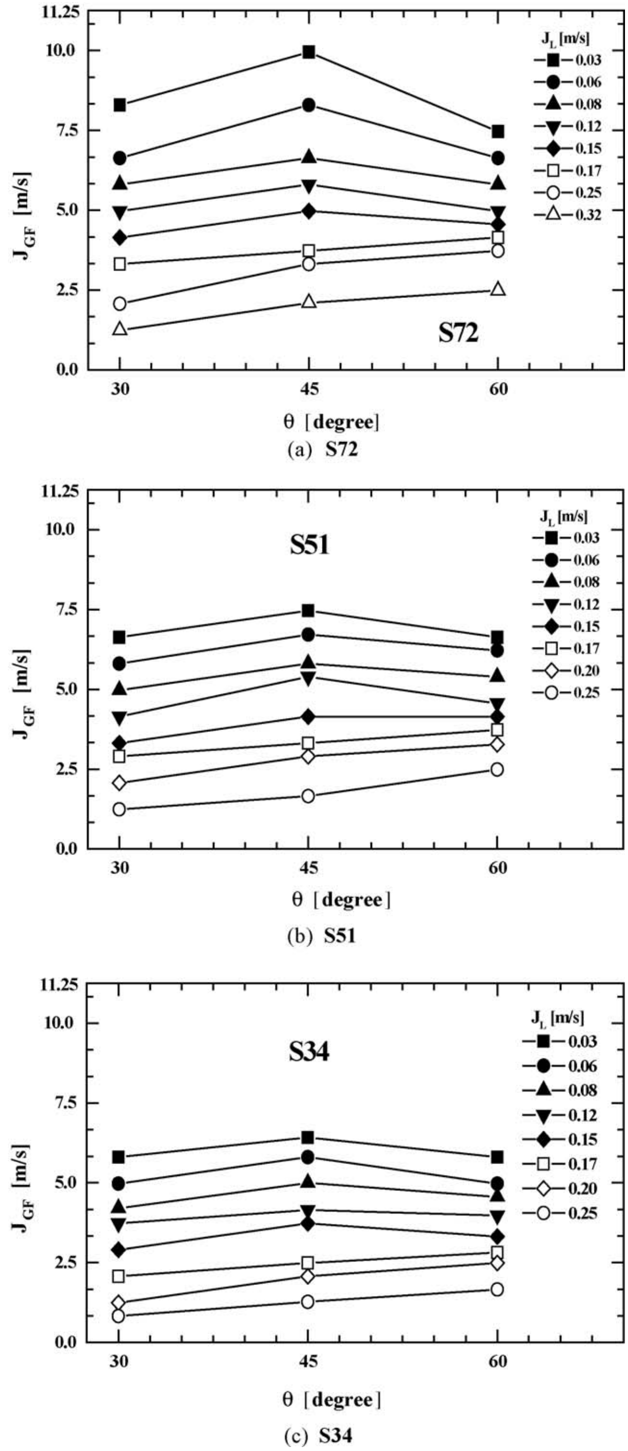

Fig. 4. Effect of pipe inclination on J_{GF} ($L = 1.1$ m).

3.2.2. Effect of pipe length

In Fig. 5, the flooding gas velocity J_{GF} is plotted against the pipe length L, (a), (b) and (c) being for the pipe inclination $\theta = 30°$, 45° and 60°, respectively. And the inlet superficial liquid velocity J_L is the parameter. The liquid is S72 and the pipe length is 1.1 m, as an example. With increasing pipe lengths, J_{GF} decreases in any conditions of J_L and pipe inclinations θ. It can be explained that the scale of the wave, i.e., the local maximum liquid hold-up at each position increases with downward movement before the onset of flooding as shown in Fig. 6. Here the flow conditions are $J_L = 0.03$ m/s, $J_G = 7.46$ m/s, $L = 1.1$ m and $\theta = 30°$. In this figure, it is shown that a wave marked as W is formed near the top of the test pipe ($x/L = 0.75$) at approximately 4.53 s for example. The local liquid hold-up of this wave is 0.08 at the onset. This wave propagates downward accompanying the increase of height and scale of the wave. Then the local liquid hold-up of this wave becomes 0.36 near the lower end of the pipe, $x/L = 0.25$. From this result an assumption can be made as follow. Under the same condition of the both flow rates before the onset of flooding, the maximum liquid hold-up increases with the pipe length. The higher the maximum liquid hold-up, the smaller the gas flow area in the pipe, and the higher the drag force at the interface. The breakdown of the wave as a characteristic of flooding occurs easily if the drag force is high. Therefore, the flooding takes place in the lower superficial gas velocity if the pipe length is long. However, the present phenomena are contradictory to that of Dukler et al. (1984). The difference in the results is considered as follow, i.e., they used the sudden expansion at the liquid outlet in their experiments, in which it produces a large perturbation near the water outlet.

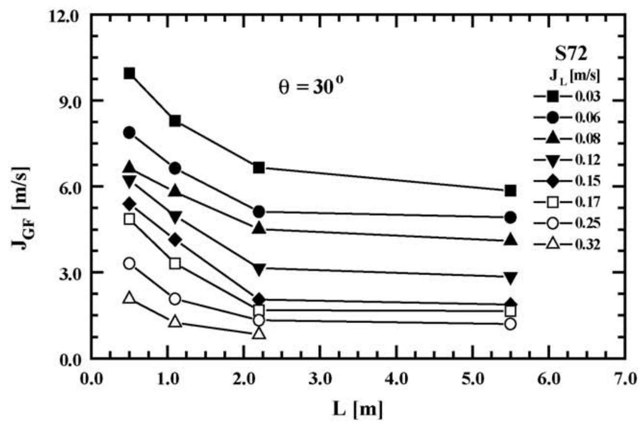

(a) θ=30°

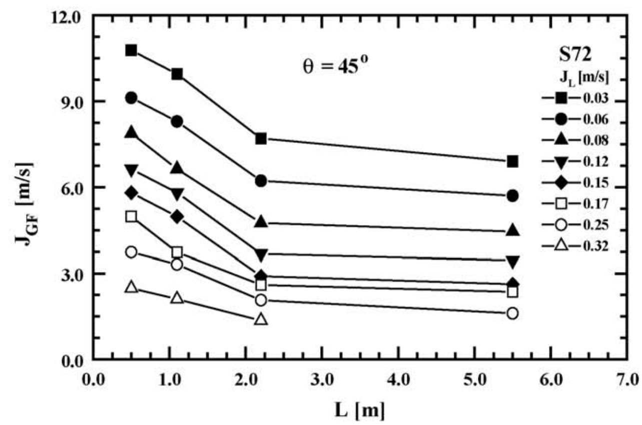

(b) θ=45°

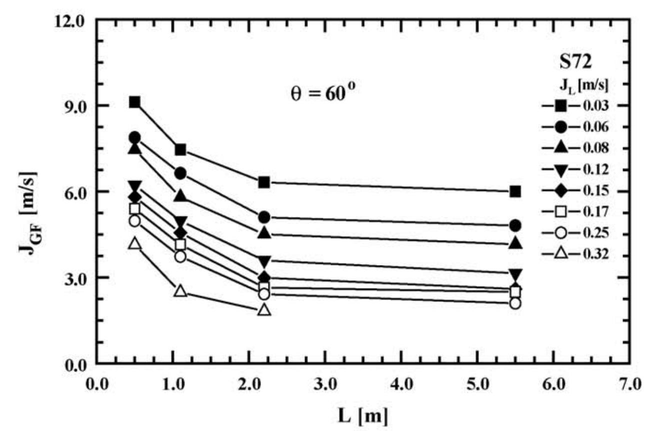

(c) θ=60°

Fig. 5. Effect of pipe length on J_{GF} (S72, D = 16 mm).

Therefore, it was considered that the effect of pipe length on J_{GF} could not be found in their experiments.

It is found that the pipe length affects flooding mechanisms. Fig. 7 shows the area map of existing the lower flooding (LF) and the upper flooding (UF). It is clearly shown that the upper flooding region decreases as the pipe length decreases. If the pipe diameter was 16 mm, it was found that the upper flooding could not be observed when the pipe length was 0.5 m. From this figure it is concluded that the flooding mechanism changes from upper to lower flooding, that means the blockage of liquid

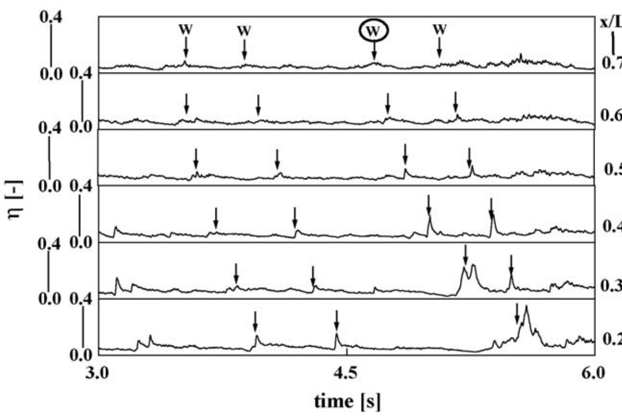

Fig. 6. Growing process of large wave before the onset of flooding (J_L = 0.03 m/s, J_G = 7.46 m/s, L = 1.1 m and θ = 30°).

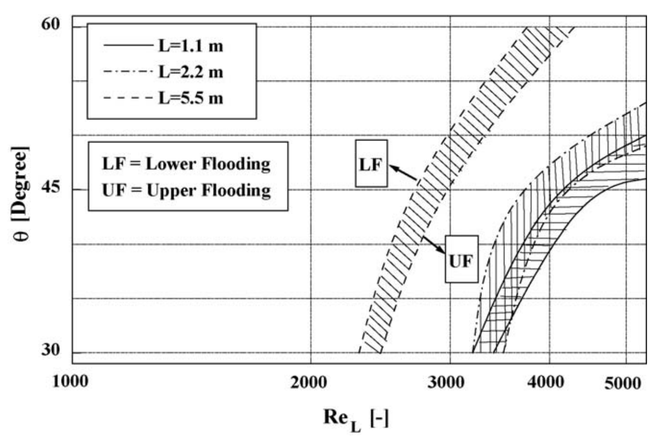

Fig. 7. Map of flooding mechanisms (D = 16 mm).

slug in the upper part of the pipe is swept out, in high liquid flow rates and for shorter pipes.

3.2.3. Effect of pipe diameter

The typical effect of the pipe diameter on J_{GF} is presented in Fig. 8. The pipe length was 5.5 m and the liquid was S72. As shown in this figure, J_{GF} decreases gradually with J_L, J_{GF} in the

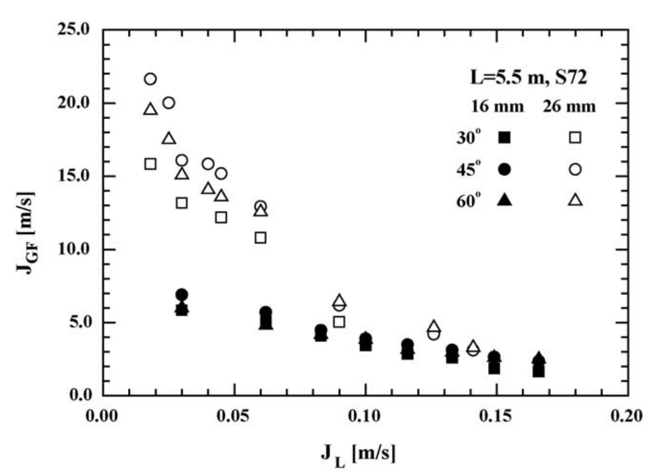

Fig. 8. Effect of pipe diameter on J_{GF} (L = 5.5 m, S72).

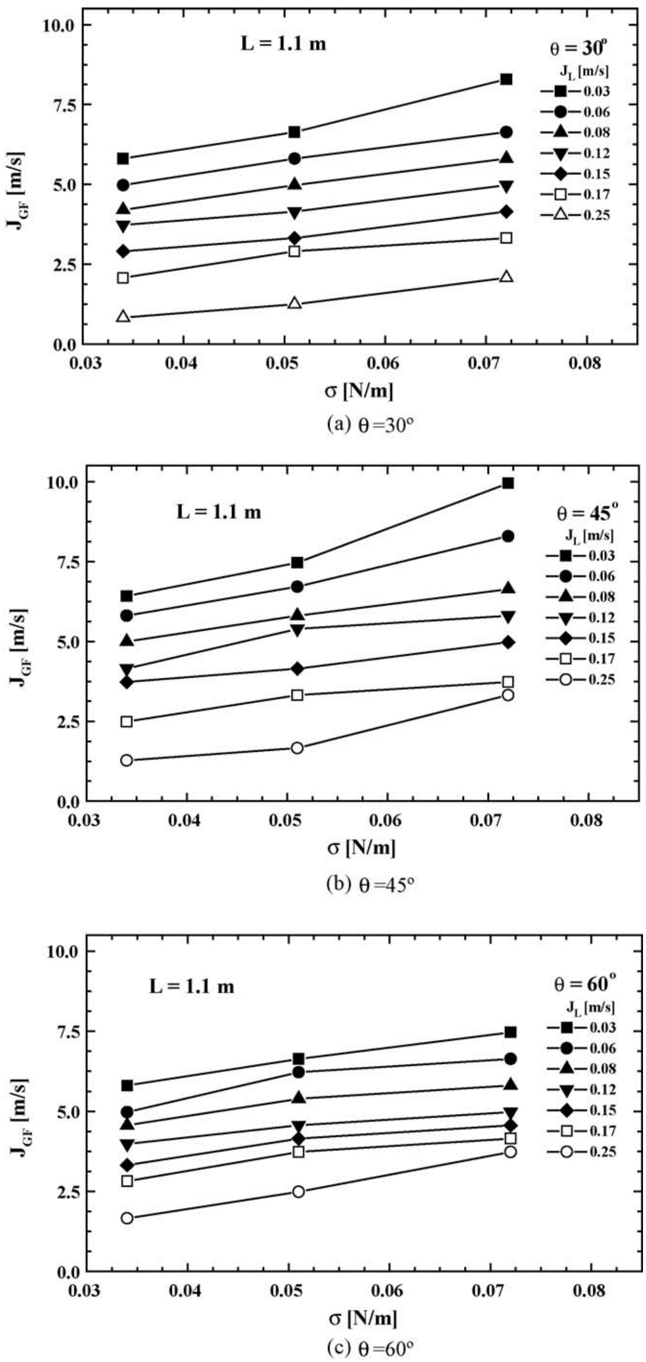

Fig. 9. Effect of surface tension on J_{GF} ($L = 1.1$ m).

case of $D = 26$ mm is larger than that of $D = 16$ mm, the difference becomes small with increasing J_L, and then it gradually approaches zero near $J_L = 0.15$ m/s.

3.2.4. Effect of liquid surface tension

Fig. 9(a)–(c) shows the typical results of the effect of the surface tension on J_{GF}, (a), (b) and (c) being for $\theta = 30°$, 45° and 60°, respectively. In the figure, J_{GF} is plotted against the surface tension σ. The inlet superficial liquid velocity J_L is the parameter. Here the pipe length is 1.1 m, as an example. Close inspection of the figure reveals that J_{GF} increases with the surface tension for all the examined pipe inclinations. In the previous paper, the present authors (Deendarlianto et al., 2004) reported that before the onset of flooding, the maximum liquid hold-up increases as the surface tension decreases for given air and liquid flow rates, and it relates to the gas flow area in counter-current two-phase flow. The larger the liquid hold-up, the larger the drag force between gas and liquid. Therefore, the flooding will occur at a smaller gas flow rate in the case of smaller surface tension. This trend is similar to those by Chung et al. (1980) and English et al. (1963) who examined that relation in vertical pipes.

Regarding flooding mechanisms, it is observed that surface tension also affected the flooding mechanisms in high liquid flow rates. From the visual observation and the analysis of the time variations of liquid hold-up at the onset of flooding, we found that in high liquid flow rate the flooding mechanism changes from upper flooding to lower flooding as the surface tension decreases. This is due to the difference of interfacial behavior of the liquid film near the liquid inlet. The examples of interfacial behavior of the liquid film under the same liquid flow rate are shown in Fig. 10(a) and (b) for S72 and S51, respectively. In the case of S72, large waves with short wave lengths were observed in low gas flow rate. An increase in the gas flow rate causes further wave growth and the wave blocks the cross section i.e., it became a liquid slug in the upper part of the pipe. The occurrence of blockage process is shown clearly in Fig. 10(a).

The decrease of surface tension from S72 to S51 changes the liquid slug to the ring-type waves near the liquid inlet. This is shown clearly in Fig. 10(b). The sign of RW indicates the occurrence of this wave. This ring-type wave is maintained for some distance (6.25–11.25)D and then quickly drains down along the wall of the pipe forming a stratified wavy layer. The maximum liquid hold-up of this wavy layer increases with downward movement. In this condition, the maximum of liquid hold-up at the lower part of the test pipe is higher than the upper part. Therefore, the breakdown of the wave occurred at the lower part of the test pipe, i.e., the lower flooding.

3.3. Examination of existing correlations

Wallis (1969) investigated the initiation of flooding in vertical pipes and proposed the dimensionless number, J_K^*, in terms of the gas and liquid superficial velocities. It is defined as follows:

$$J_K^* = J_K \sqrt{\frac{\rho_K}{gD(\rho_L - \rho_G)}} \tag{1}$$

where, subscript K indicates gas and liquid phases, ρ the density and D is the pipe diameter. The correlation is expressed as,

$$(J_G^*)^{1/2} + m(J_L^*)^{1/2} = C \tag{2}$$

The constants m and C were determined by experiments and no theoretical basis was given for the use of the above correlation. For smooth outlet and inlet condition of liquid, Eq. (2) was modified by Dukler and Smith (1979) as follows:

$$(J_G^*)^{1/2} + (J_L^*)^{1/2} = 0.88 \tag{3}$$

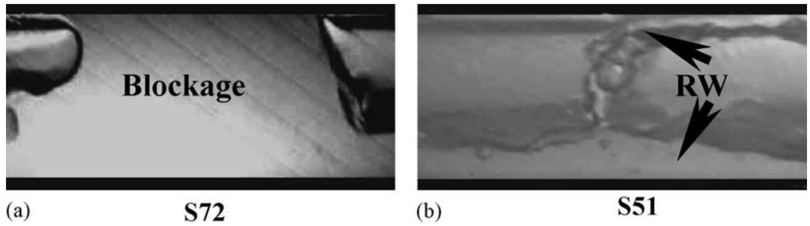

Fig. 10. Interfacial behavior of liquid film at the onset of flooding near the liquid inlet ($J_L = 0.25$ m/s, $\theta = 30^\circ$ and $L = 1.1$ m).

Parallel to this work Pushkina and Sorokin (1969) also investigated the stability of counter-current two-phase flow in vertical pipes and suggested a similar empirical correlation in terms of the Kutateladze number of gas and liquid phase, K_G and K_L, defined as below:

$$K_G^{1/2} + mK_L^{1/2} = C_K \tag{4}$$

where K_G and K_L are defined by $K_G = J_{GF}\rho_G^{1/2}[g\sigma(\rho_L - \rho_G)]^{-1/4}$ and $K_L = J_L\rho_L^{1/2}[g\sigma(\rho_L - \rho_G)]^{-1/4}$, respectively, and C_K is a constant. They proposed $m = 0$ and $C_K = 3.2$, independent of the pipe diameter. This independency on pipe diameter is contrary to Wallis correlation as written in Eq. (1). For this reason Tien et al. (1979) conducted air–water tests for four different pipe diameters: 15.9, 31.8, 46.0 and 69.9 mm. The onset of flooding was determined visually. Their experimental results indicate that the initiation of flooding is strongly affected by the pipe diameter. The flooding gas velocity increases with the pipe diameter. Recently Jayanti et al. (1996) performed a computational fluid dynamic (CFD) study and found also the same conclusion. Finally Tien et al. improved the correlation proposed by Pushkina and Sorokin as follows:

$$K_G^{1/2} + mK_L^{1/2} = C_1 \tanh\{C_2 D^{*1/4}\} \tag{5}$$

where

$$D^* = D\left\{\frac{g(\rho_L - \rho_G)}{\sigma}\right\}^{1/2} \tag{6}$$

here, $m = 0.65$–0.8, $C_1 = 1.79$–2.1 and $C_2 = 0.8$–0.9.

Figs. 11 and 12 show the onset of flooding data plotted in terms of the dimensionless parameters proposed by Wallis and Kutateladze, respectively. It is noted that:

(1) From Fig. 11, it is revealed that the present experimental data scatter widely on this map. This signifies that the surface tension and the pipe length are important factors to correlate the flooding data. Next, the Wallis' dimensionless number also fails to correlate the data of different pipe diameters although it is included in the parameter. The straight line in Fig. 11 is the flooding limit for vertical pipes according to the Dukler and Smith correlation (Eq. (3)). This result demonstrated that the flooding gas velocity in vertical pipes is lower than that of inclined pipes.
(2) From Fig. 12, Tien et al. correlation gives a better agreement but not satisfactory approximation. This correlation can account for the effect of the surface tension, but not for the effect of pipe diameter, although it is included in the equation. In comparison with the Wallis dimensionless number, the scattering of the data is reduced by using this correlation.

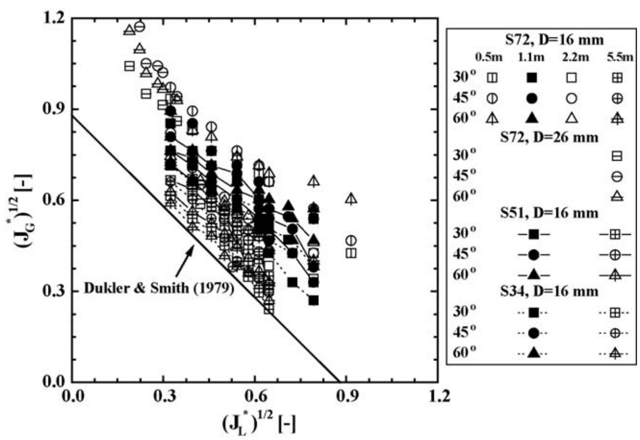

Fig. 11. Correlation of the present experimental data with Wallis dimensionless number.

Barnea et al. (1986) successfully adopted the Taitel and Dukler (1976) model to predict the flooding gas velocity in an inclined pipe. This model is based on the steady-state momentum equation for the liquid and gas phases. The growth of a solitary wave in stratified flow during the slug formation in co-current two-phase flow and the condition of no solution for equilibrium counter-current flow were used as the flooding criterion. Although the dependence on the pipe inclination in this model

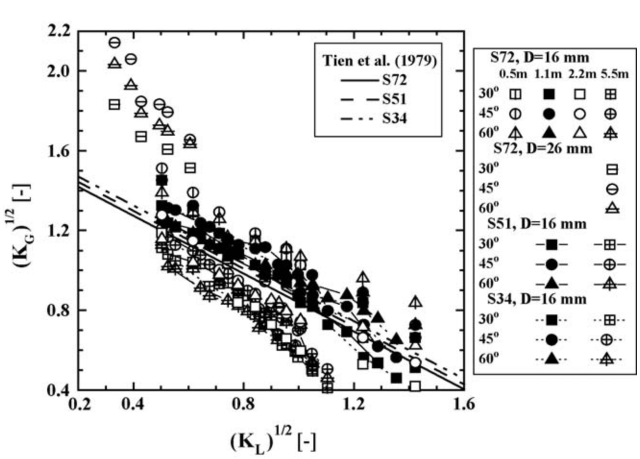

Fig. 12. Correlation of the present experimental data with Kutateladze dimensionless number.

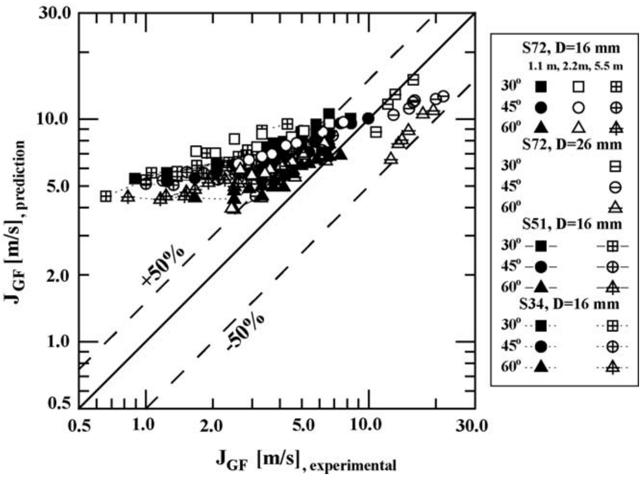

Fig. 13. Comparison of the present experimental data with Taitel and Dukler model.

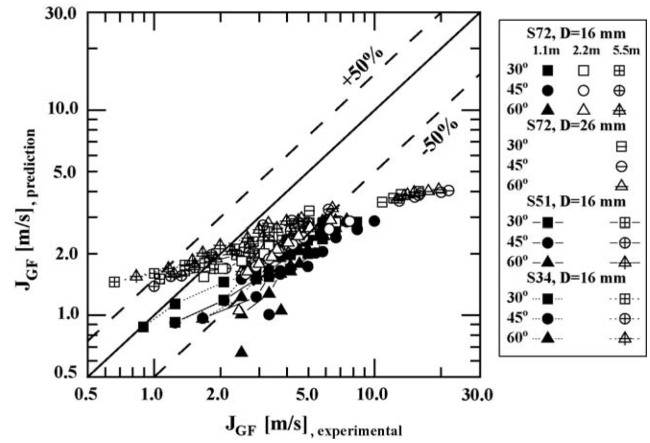

Fig. 14. Comparison of the present experimental data with Zapke and Kroger correlation.

is valid only for relatively small angles of inclination, where the flow pattern remains stratified, it was considered applicable to the present experiment.

A comparison between the experimental data and the Taitel and Dukler model is given in Fig. 13. The model overpredicts the flooding gas velocity. The difference between the prediction and the experimental data increases as the surface tension decreases and the pipe length increases. This is because those parameters are not taken into consideration in this model. In fact, the pipe length and the surface tension play an important role on the flooding gas velocity.

Zapke and Kroger (2000) examined the counter-current gas–liquid flow in inclined ducts. They noted that the flooding gas velocity J_{GF} increases with the duct height. They also recommended using the Ohnesorge number to account for the terms of liquid properties on the gas velocity at the onset of flooding. It is defined as follows:

$$Oh_L = \sqrt{\frac{\mu_L^2}{\rho_L D_e \sigma}} \tag{7}$$

In Eq. (7) μ_L is the liquid viscosity, σ the surface tension, and D_e is the hydraulic diameter. Zapke and Kroger also claimed that their correlation could be used to predict J_{GF} in inclined pipes, although it was developed for inclined rectangular ducts. In Fig. 14, a comparison between the experimental data and the Zapke and Kroger correlation is presented. Close inspection of this figure reveals that the correlation of Zapke and Kroger agrees well with the experimental data when the surface tension is low. The predicted values are systematically lower than the experimental data. Especially when the surface tension and the pipe diameter are larger the liquid film becomes thin, therefore J_{GF} becomes large. Thus the prediction results in large error. Furthermore, the data of different pipe lengths are not also correlated well because the effect of pipe length is not considered in this correlation.

Recently Fiedler and Auracher (2004) performed an experimental and theoretical investigation of reflux condensation in an inclined small diameter tube. They reported that the flooding correlation by English et al. showed the best agreement with their own experimental data. However, they do not take into account the effect of the inclination angle θ, therefore a term was added to consider the pipe inclination as follows:

$$J_{GF} = 0.45(\sin 1.7\theta)^{0.38} \frac{d^{0.322} \rho_L^{0.419} \sigma^{0.097}}{\rho_G^{0.462} \mu_L^{0.15} J_L^{0.075}} \tag{8}$$

A comparison between the experimental data and the correlation proposed by Fiedler and Auracher is presented in Fig. 15. It is noteworthy that the predictions by Fiedler and Auracher are relatively poor. The poor prediction seems to be related to the effect of condensation on their experiment. While, the present data was taken under an adiabatic condition.

3.4. Correlation development

A flooding correlation corresponding to the lower flooding only was developed in the present research. Correlation development for the upper flooding did not carry out here because data obtained were limited. The important conception in establish a new correlation is as follows:

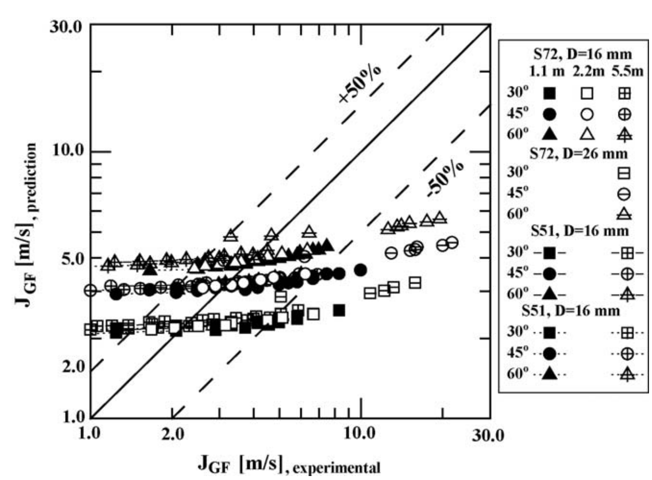

Fig. 15. Comparison of the present experimental data with Friedler and Auracher correlation.

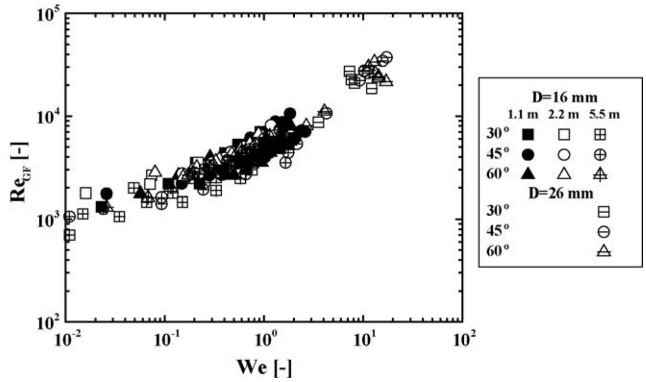

Fig. 16. Relation between Weber number and the gas Reynolds number at the onset of flooding.

(1) The flooding gas velocity J_{GF} is observed as an inverse proportion to the superficial liquid velocity ($J_{GF} \propto J_L^{-a}$). This effect is included in Reynolds numbers Re_K of both phases in the proposed correlation, where:

$$Re_K = \frac{\rho_K J_K D}{\mu_K} \tag{9}$$

(2) As shown in Section 1, the breakdown of wave is considered as the onset of flooding, and we observed that the entrainment of liquid droplet arises nearly at the same time of the breakdown of the wave. For this reason, the Weber number, We, as a ratio of shear force to surface tension force is used which is defined as below in the present study:

$$We = \frac{\rho_G (\Delta v)^2}{\sigma / h} \tag{10}$$

where, $\Delta v = \left(\frac{J_{GF}}{\alpha} - \frac{J_L}{\eta}\right)$ indicates the relative velocity between both phases and h the wave height. Here the wave height h is calculated from the liquid hold-up data. According to our experimental result this dependence can be expressed by an expression of the form $Re_{GF} \propto We^m$ as is shown in Fig. 16.

(3) The pipe inclination effect is expressed as $g \sin\theta$, so the modified Froude number Fr_L is defined as follows:

$$Fr_L = \frac{J_L^2}{(g \sin\theta) D} \tag{11}$$

(4) The effect of the pipe diameter is accounted by using Froude number. According to the experimental data the gas Reynolds number at the onset of flooding Re_{GF} is proportional to Fr_L^{-b} as shown in Fig. 17.

(5) The effect of pipe length is taken into account in the expression of L/D.

From the above consideration, a correlation for Re_{GF} is expressed as a function in the next expression.

$$Re_{GF} = f(Re_L, We, Fr_L, L/D) \tag{12}$$

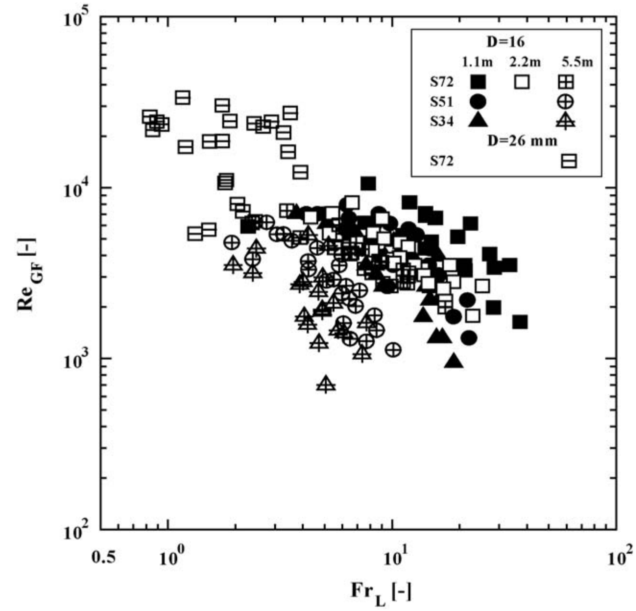

Fig. 17. Relation between the liquid Froude number and the gas Reynolds number at the onset of flooding.

By trial and error we obtained Eq. (13) to predict the flooding gas velocity in inclined pipes.

$$Re_{GF} = 1.35 \times 10^4 \, Re_L^{-0.12(L/D)^{0.01}} \, We^{0.55} \, Fr_L^{-0.01} \tag{13}$$

As seen from Fig. 18, the present correlation Eq. (13) estimates Re_{GF} with the accuracy of ±35% without clear systematic error. In addition the overall performance of this correlation is better than the existing correlations discussed above.

We also tried to correlate the experimental data by modifying the Wallis correlation, in which the parameters of pipe inclination, pipe length and surface tension were accounted in the constants C and m. However, it produced a complicated equation and it does not useful in practical application. On the other hand, it also could not express the physical meaning of the wave breakdown at the onset of flooding. Therefore, we proposed Eq. (13), in which the physical meaning of wave breakdown as the

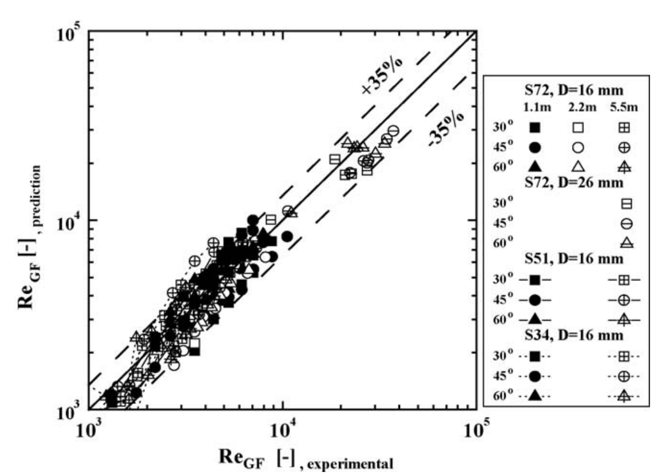

Fig. 18. Correlation of the present experimental data with Eq. (13).

ratio of shear force to surface tension force is expressed as Weber number.

4. Conclusions

An experiment was carried out in the adiabatic counter-current gas–liquid two-phase flow in inclined pipe with the inner diameters of 16 and 26 mm for the pipe length of 0.5, 1.1, 2.2 and 5.5 m. Pipe inclinations were 30°, 45° and 60° to horizontal. The working fluids were air–water and air–aqueous oleic acid natrium solution systems. The purpose of the present study is to clarify experimentally the effects of pipe inclination, pipe length, pipe diameter and liquid surface tension on the flooding gas velocity in inclined pipe and to propose a correlation of it. The main results are summarized as follows:

(1) The flooding gas velocity takes a maximum value at approximately 45 ° pipe inclination in the case of low superficial liquid velocity. Meanwhile, it moves to a higher pipe inclination in the case of higher liquid region.
(2) The flooding gas velocity decreases as the pipe length decreases, while it increases with the pipe diameter. The effect of pipe diameter is significant at low inlet superficial liquid velocity.
(3) From the observations of the shape of the waves from visual observation and the time variations of liquid hold-up, it is clarified that the interfacial structure between gas and liquid phases at the onset of flooding is strongly dependent on the surface tension, signifying that the flooding gas velocity decreases with the surface tension.
(4) We proposed Eq. (13) to correlate the flooding gas velocity in inclined pipes, in which the effects of the pipe inclination, pipe length, pipe diameter and surface tension are taken into consideration.

Acknowledgements

The authors would like to thanks Mr. Keisuke Konishi and Mr. Masafumi Konishi, the graduate students of the mechanical engineering of Tokushima University at that time for their cooperation in the experiment and technician Jiro Yamasita, for the manufacture of the experimental devices.

References

Barnea, D., Ben Yoseph, N., Taitel, Y., 1986. Flooding in inclined pipe: effect of entrance section. Can. J. Chem. Eng. 64 (2), 177–184.
Celata, G.P., Cumo, M., Setaro, T., 1992. Flooding in inclined pipes with obstructions. Exp. Therm. Fluid Sci. 5, 18–25.
Chung, K.S., Liu, C.P., Tien, C.L., 1980. Flooding in two-phase counter-current flow. II. Experimental investigation. Physicochem. Hyd. J. 1, 209–220.
Clift, R., Pritchard, C., Nedderman, R.M., 1966. The effect of viscosity on the flooding conditions in wetted wall columns. Chem. Eng. Sci. 21, 87–95.
Deendarlianto, Ousaka, A., Kariyasaki, A., Kusano, K., 2002. Flooding phenomena for air–water two-phase flow in inclined pipe: effect of pipe inclination on the onset of flooding. In: Proceedings of the 5th JSME-KSME Fluids Engineering Conference, Paper No. 10j_11, Nagoya, Japan (CD-ROM).
Deendarlianto, Ousaka, A., Kariyasaki, A., Fukano, T., Konishi, M., 2004. The effects of surface tension on the flow pattern and counter-current flow limitation (CCFL) in gas–liquid two-phase flow in an inclined pipe. Jpn. J. Multiphase Flow 18 (4), 337–350.
Deendarlianto, Ousaka, A., Kariyasaki, A., Fukano, T., 2005a. Investigation of liquid film behavior at the onset of flooding during adiabatic counter-current air–water two-phase flow in an inclined pipe. Nucl. Eng. Design 235, 2281–2294.
Deendarlianto, Ousaka, A., Kariyasaki, A., Fukano, T., 2005b. Experimental study on the liquid film characteristics at the onset of flooding in an inclined pipe. In: Proceedings of the 6th JSME-KSME Thermal and Fluids Engineering Conference, Paper No. JC.07, Jeju, Korea (CD-ROM).
Dukler, A.E., Smith, L., 1979. Two-phase interactions in counter-current flow: studies of the flooding. USNRC, NUREG/CR-0617.
Dukler, A.E., Smith, L., Chopra, A., 1984. Flooding and upward film flow in tube. Int. J. Multiphase Flow 10 (5), 585–597.
English, K.G., Jones, W.T., Spillers, R.C., Orr, V., 1963. Flooding in a vertical updraft partial condenser. Chem. Eng. Prog. 59 (7), 51–54.
Fiedler, S., Auracher, H., 2004. Experimental and theoretical investigation of reflux condensation in an inclined small diameter tube. Int. J. Heat Mass Transfer 47 (20), 4031–4043.
Fukano, T., 1971. Characteristics of pulsation of gas–liquid two-phase upward flow. Dr. Thesis. Kyushu University (in Japanese).
Fukano, T., 1998. Measurement of time varying thickness of liquid film flowing with high speed gas flow by a constant electric current method (CECM). Nucl. Eng. Design 184, 363–377.
Hewitt, G.F., 1977. Influence of end conditions, tube inclination and physical properties on flooding in gas–liquid flow. UKAEA Report HTFS-RS222.
Jayanti, S., Tokarz, A., Hewitt, G.F., 1996. Theoretical investigation of the diameter effect on flooding in counter-current flow. Int. J. Multiphase Flow 22 (2), 307–324.
Jeong, J.H., No, H.C., 1996. Experimental study of the effect of pipe length and pipe end geometry on flooding. Int. J. Multiphase Flow 22 (3), 499–514.
Kamei, S., Onishi, J., Okane, T., 1954. Flooding in a wetted wall tower. Chem. Eng. 18, 364–368 (in Japanese).
Matsuki, H., Kaneshina, S., Yamashita, Y., Motomura, K., 1994. Automatic surface tension measurements of aqueous surfactant solutions by the drop volume method. Langmuir 10 (11), 4394–4396.
Matsuki, H., Yamashita, Y., Kaneshina, S., 1999. Development of automatic interfacial tension measurement apparatus based on the drop volume method. J. Jpn. Oil Chem. Soc. 48 (11), 57–64 (in Japanese).
McQuilland, K.W., Whalley, P.B., 1985. Flooding in vertical two-phase flow. Int. J. Multiphase Flow 11 (6), 741–760.
Mouza, A.A., Paras, S.V., Karabelas, A.J., 2003. Incipient flooding in inclined tubes of small diameter. Int. J. Multiphase Flow 29 (9), 1395–1412.
Pushkina, O.L., Sorokin, L., 1969. Breakdown of liquid film motion in vertical tubes. Heat Transfer Sov. Res. 1, 56–64.
Suzuki, S., Ueda, T., 1977. Behavior of liquid films and flooding in counter-current two-phase flow. Part I. Flow in circular tubes. Int. J. Multiphase Flow 3 (6), 517–532.
Taitel, Y., Dukler, A.E., 1976. A model for predicting flow regime transition in horizontal and near horizontal gas–liquid flow. AIChE J. 22, 47–55.
Tien, C.L., Chung, K.L., Liu, C.P., 1979. Flooding in two-phase counter-current flows. EPRI Report No. EPRI NP-1283.
Wallis, G.B., 1969. One-dimensional Two-phase Flow. Mc Graw Hill, New York, pp. 336–345.
Zabaras, G.J., Dukler, A.E., 1988. Counter-current gas–liquid annular flow, including the flooding state. AIChE J. 34 (3), 389–396.
Zapke, A., Kroger, D.G., 2000. Counter current gas–liquid flow in inclined and vertical ducts. I. Flow patterns, pressure drop characteristics and flooding. Int. J. Multiphase Flow 26 (9), 1439–1455.